AGU ADVANCING EARTH AND SPACE SCIENCES

Geophysical Research Letters

RESEARCH LETTER
10.1029/2024GL110126

Channel-Spanning Logjams and Reach-Scale Hydraulic Resistance in Mountain Streams

Elizabeth Follett[1] and **Ellen Wohl**[2]

[1]Department of Civil & Environmental Engineering, University of Liverpool, Liverpool, UK, [2]Department of Geosciences, Colorado State University, Fort Collins, CO, USA

Key Points:

- We compared the hydraulic impact of logjams, identified by effective resistance, across 37 reaches and 11 years in the Colorado Rockies
- Effective resistance increases with decreasing stream power, analytically linked to dependence on jam structure and spacing
- Observed random jam distribution reduces effective resistance compared to uniform distribution, due to backwater truncation

Supporting Information:

Supporting Information may be found in the online version of this article.

Correspondence to:

E. Follett,
e.follett@liverpool.ac.uk

Citation:

Follett, E., & Wohl, E. (2024). Channel-spanning logjams and reach-scale hydraulic resistance in mountain streams. *Geophysical Research Letters*, *51*, e2024GL110126. https://doi.org/10.1029/2024GL110126

Received 3 MAY 2024
Accepted 14 AUG 2024

Abstract Logjams create an upstream backwater of deepened, slower water, locally reducing bed shear stress. We compared hydraulic impact of logjam series across 37 geomorphically diverse reaches of mountain streams observed over 11 years in the US Southern Rockies. To enable reach-scale comparison of logjam structure and spacing, we identified the modeled best-fit effective resistance coefficient minimizing difference between outflow exiting a 1D channel with logjams present, and the same model channel with elevated channel resistance. Effective resistance increased with ratio of jam upstream depth to depth without a logjam, ratio of backwater length to average spacing, and decreased for randomly distributed jams due to close spacing, which reduced backwater impact. An analytic approximation and boundaries for region of relative spacing with steepest increase in effective resistance are provided. Our results can assist in targeting interventions to areas where hydraulic impact is greatest, providing value for money in nature-based solution design.

Plain Language Summary In a river channel, logjams created by wood pieces create upstream backwater regions with slower, deepened water. By creating a backwater, logjams increase heterogeneity of habitat and sediment transport and increase connection between river channel and floodplain. We compared logjams in 37 reaches of mountain streams in the US Southern Rockies. The sites studied had high variation in logjam density, channel steepness, channel width, and floodplain width. To compare between reaches and identify the ability of logjam backwaters to slow water within a river channel, we found an effective channel resistance coefficient that produced similar model output as a reach containing a series of logjams. The effective resistance increased with ratio of jam upstream depth to flow depth without a logjam, and ratio of backwater length to average spacing. The highest rate of increase in effective resistance with more logjams in the river reach occurs for an intermediate range of inter-jam spacing relative to backwater length. Engineered logjam and wood addition projects could target this range to provide the most benefit per intervention.

1. Introduction

1.1. Large Wood, Logjams, and River Management

River scientists and managers have increasingly recognized beneficial effects of large wood (pieces ≥1 m long and 10 cm diameter) in river channels and floodplains (Swanson et al., 2020; Wohl, 2017). Forested river corridors in temperate latitudes are relatively depauperate in large wood due to centuries of deforestation, channel engineering, and active wood removal (Montgomery et al., 2003; Wohl, 2014). River management in many regions now emphasizes wood reintroduction and retention to restore lost functions associated with wood (Grabowski et al., 2019), including increased hydraulic roughness and lateral connectivity between channel and floodplain; attenuation of downstream fluxes of water, solutes, sediment, and organic matter; greater spatial heterogeneity of hydraulics, substrate, and channel bedforms and planforms; and enhanced habitat abundance and diversity and biomass and biodiversity (Deane et al., 2021; Gregory et al., 2003; Gurnell et al., 2005; Ruiz-Villanueva et al., 2016). Logjams that span the bankfull channel can be disproportionately effective in creating these functions (Livers & Wohl, 2021; Mao et al., 2008; Welling et al., 2021). Low-tech process-based restoration measures such as installation of beaver dam analogs and engineered logjam leaky barriers for fish habitat and natural flood management commonly need to balance desired functions with site accessibility, cost, potential hazards to recreational users, hazards associated with increased overbank inundation or channel mobility, or hazards to downstream infrastructure from mobile wood pieces (Pess et al., 2011; Polvika & Claeson, 2020; Roni et al., 2015; Wohl et al., 2016).

Channel-spanning logjams create an upstream backwater of slower, deepened water, increasing flow heterogeneity, capture of bedload and suspended sediment, and lateral connectivity (Bilby, 1981; Bouwes et al., 2018; Livers & Wohl, 2021; Schalko et al., 2018). The extent of increase in upstream backwater depth, which rises to balance the drag generated by water flowing past jam elements, is proportional to the number, size, and packing density of the logs, which comprise a dimensionless structural metric (Follett et al., 2020). Channel-spanning logjams can create sufficient channel blockage and upstream deposition to enhance overbank flow (Brummer et al., 2006). Overbank flow can concentrate, increase shear stress on the floodplain, and initiate formation of new secondary channels, leading to a multithread channel planform (Livers et al., 2017; Sear et al., 2010; Wohl, 2011). Historic loss of wood within river corridors likely contributed to channel planform simplification to single-thread configuration compared to historic prevalence, along with channelization and bank stabilization for flood control and navigation (Brown et al., 2018; Collins et al., 2002, 2003, 2012; Pišút, 2002).

We compare the hydraulic impact of channel-spanning logjam structure and spacing across 38 geomorphically diverse reaches of mountain streams in the US Southern Rockies (Figures 1a–1c; map of site spatial arrangement shown in Figure 1 in Wohl & Iskin, 2022). This unmanaged system provides an ideal data set to explore variation of logjam properties with channel characteristics such as channel slope S, channel bankfull width B_{BF} and depth H_{BF}, bed resistance C_f, and valley confinement B_{fp}/B_{BF} (Wohl & Iskin, 2022). Wood size is limited due to pressures of insects, fire, and water scarcity, resulting in high wood mobility and high jam transience compared to lowland areas (Collins et al., 2012). The logjams observed in this system are highly transient, with mean persistence of 1.5–2 years (Wohl & Iskin, 2022). Two-way interaction between jams, channel, and floodplain characteristics occurs throughout the jam persistence cycle (Figure 1d). Jam occurrence was randomly distributed at the reach scale, linked to tree fall near channel banks and ratio of wood piece length to channel width. Jam formation and dissolution typically occurs during annual spring snowmelt flows (Wohl & Scamardo, 2021). Jams which break apart release wood pieces for further transport to the local floodplain or downstream, while persistent jams allow upstream accumulation of sediment over multiple years and may experience structural changes over time.

To enable cross-reach comparison of reach-scale series of logjams, jam hydraulic impact in the channel was identified with modeled best-fit effective resistance elevated above bed resistance with no jams present which resulted in an outflow hydrograph most closely matching the outflow from a model reach containing a series of individual logjams. The cumulative effect of multiple logjams has been modeled with an empirical increase in channel hydraulic roughness (Addy & Wilkinson, 2019; Follett and Hankin, 2022) in catchment-scale hydraulic models where implementation of logjams as individual structures is prohibitive. We use data from 4 unmanaged channels (a mainstem and 3 large tributaries) in Rocky Mountain National Park, Colorado that together drain 90 km^2 of subalpine forested terrain (Figure 1; Wohl & Iskin, 2022). Channel gradient within individual reaches ranges from 0.006 to 0.295, bankfull channel width ranges from 5 to 19.8 m, and ratio of floodplain to channel width varies from 1.1 to 11.4. Reach average inter-jam spacing of channel-spanning logjams is variable between reaches (L_s = 16.6–2,731.7 m; Figure 1). Tables of reach characteristics used in this paper are publicly available (see Data Availability Statement). This diverse data set allows us to explore whether the downstream spacing of logjams creates predictable patterns of jam hydraulic impact, identified by modeled effective flow resistance, across variable channel and valley geometry.

2. Methods

The logjams analyzed here are channel-spanning, defined as (a) including ≥3 pieces of wood in contact with each other exceeding 10 cm in diameter and 1 m in length, (b) spanning the bankfull channel width, and (c) altering the water-surface gradient across at least ¾ of wetted channel width at base flow (Wohl & Iskin, 2022). Logjams were located during late summer base flow using a handheld GPS (Garmin eTrex, maximum horizontal accuracy ±3 m). Total length of channel surveyed along each creek was subdivided into reaches (10^1–10^3 m in length) based on observed changes in primary bedforms within the active channel. Bedforms (cascade, step-pool, plane-bed, and pool-riffle; Montgomery & Buffington, 1997) in channels correlate strongly with channel gradient, bed grain size, and lateral valley confinement (Livers & Wohl, 2015). Field-designated reach boundaries were subsequently confirmed against channel gradient obtained from 1:24,000 scale topographic maps. Average bankfull channel width and floodplain width within each reach were derived from multiple field measurements using a handheld laser rangefinder (TruPulse 360B, accuracy ± 0.1 m). Floodplain boundaries were delineated in the field using combined evidence from slope gradient breaks, vegetation communities, and evidence of recent

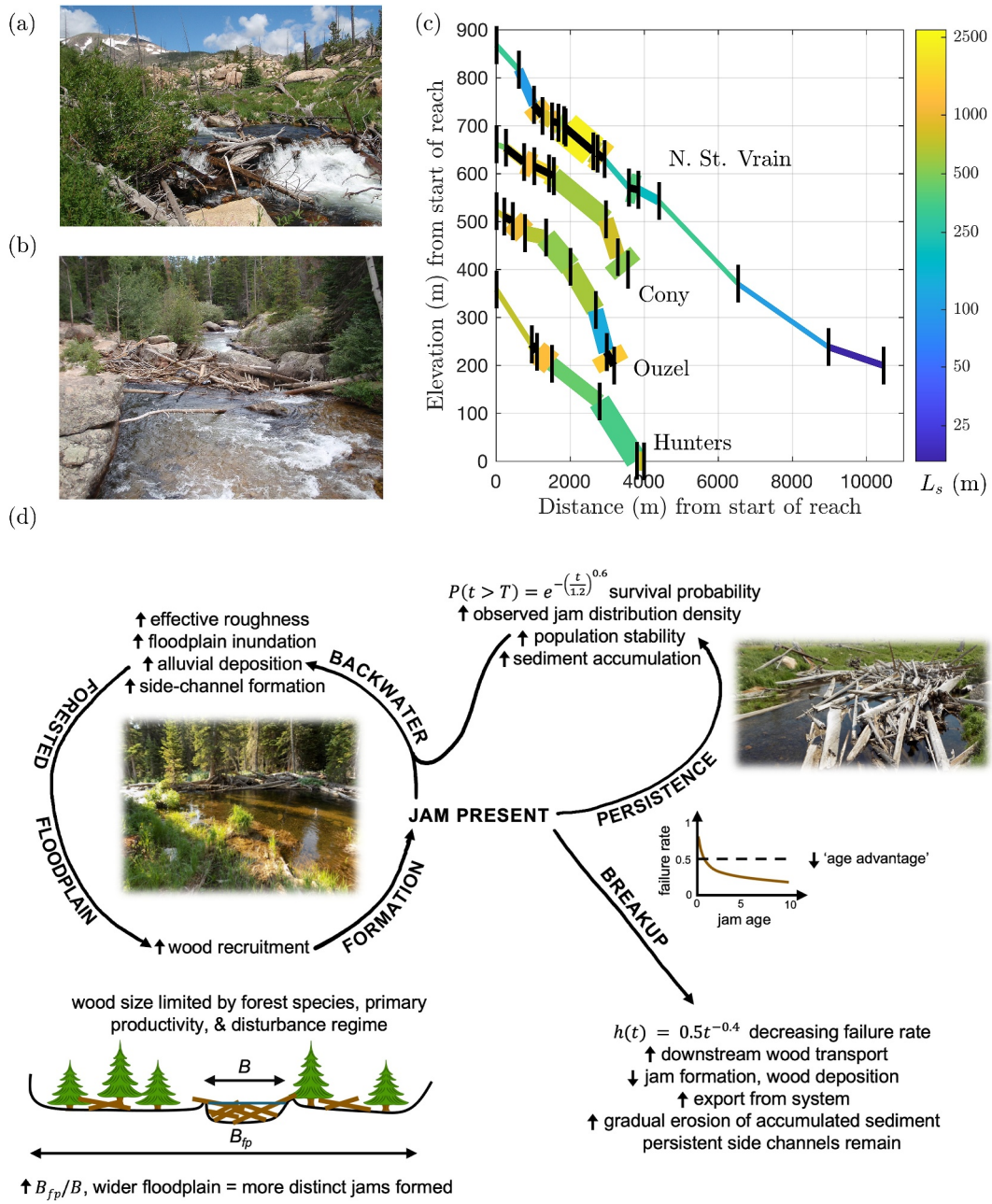

Figure 1. (a) Ouzel 6 ($L_s = 76$ m, $S = 0.064$, $B_{BF} = 10.4$ m, $B_{fp}/B_{BF} = 3.5$) (b) North St. Vrain (NSV) 15 ($L_s = 441$ m, $S = 0.054$, $B_{BF} = 18$ m, $B_{fp}/B_{BF} = 1.4$) (c) Longitudinal profile of study reaches at NSV, Cony, Ouzel, and Hunters Rivers. Line width increases with relative floodplain width. Reach boundaries shown with vertical black lines. Starting elevation of NSV, Cony, and Ouzel rivers offset upwards by 200, 400, and 200 m, respectively, in order to show difference between profiles. Reaches with observed multithread profile shown with black lines along reach profile. Increasing jam density shown by blue to yellow color gradation. (d) Schematic diagram of jam persistence cycle.

fluvial erosion and deposition. Baseflow discharge at downstream end of each reach was estimated using GPS coordinates input to the US Geological Survey StreamStats website (https://streamstats.usgs.gov/ss/). A single average value for upstream depth and bankfull depth, respectively, was used for each reach. These values were averaged from detailed measurements of 30 logjams in the study area measured within the area influenced by the logjam (Beckman, 2013; Livers Gonzalez, 2016). The primary influences on upstream water depth are jam

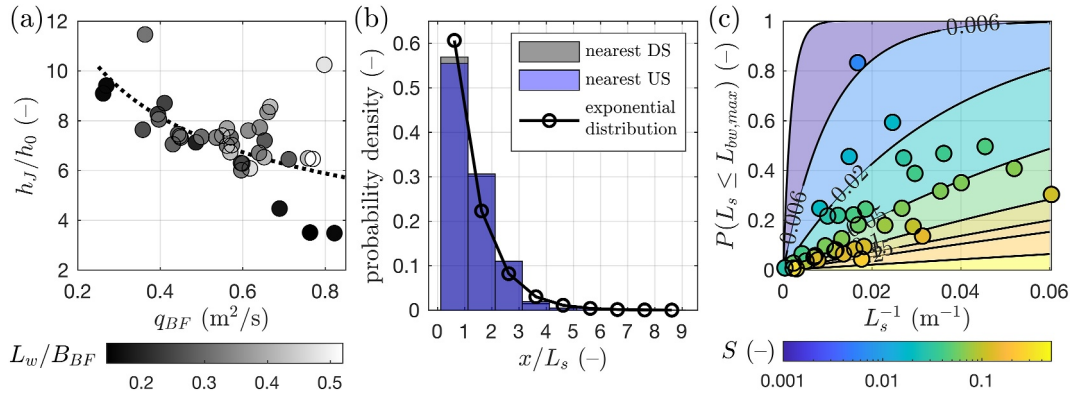

Figure 2. (a) Ratio of water depth upstream of jam to uniform flow depth h_J/h_0 with unit bankfull discharge q_{BF} (m^2/s). Dashed black line shows fit to data $h_J/h_0 = 5.3q_{BF}^{-0.47}, R^2 = 0.31$. (b) Probability density of distance to nearest upstream and downstream neighbor at exemplar site Ouzel 2 (209 jams measured over 11 years of observations), normalized by reach-average inter-jam spacing L_s (m). Exponential distribution of inter-jam spacing (Wohl & Scamardo, 2021) shown by solid black line. (c) Expected probability based on random distribution and observed S, h_J/h_0, H_{bf} (Equation 2) occurring at point of overtopping shown by circles with black outline. Contours show expected probability of jam occurrence within one backwater length for data set average $h_J/h_0 = 7$, with L_s^{-1} (m^{-1}).

characteristics (height and porosity/permeability) and reach-scale gradient. We estimated reach average water depth values based on field characterizations of jams within each reach, along with reach-scale average gradient.

The volume of water in a channel segment containing a jam at the downstream edge was related to water depths for uniform flow and the backwater sections in a 1D network model framework (see Supporting Information S1; Follett & Hankin, 2022). The asymptotic approach of the backwater curve to uniform flow depth was calculated iteratively (Chow, 1959; Julien, 1998). To find effective resistance, the maximum input discharge was chosen so that water depth upstream of a jam was at the point of overtopping ($h_J = H_{BF}$; $Q_{BF,J}$), for which the backwater length was maximum. Model input discharge was specified by a Gaussian hydrograph with $\mu = 6$ hr,$\sigma = 1$ hr, $Q_{min} = 0.5Q_{BF,J}$, and $Q_{max} = Q_{BF,J}$. Subcritical conditions were present in the jam backwater and at uniform flow for all conditions tested (Fr_J, $Fr_0 < 1$). See Table S1 in Supporting Information S1 for table of symbol definitions.

3. Results

3.1. Observed Logjam Structure and Spacing

The hydraulic impact of water flowing through a series of channel-spanning logjams in a river reach depends on spacing between jams relative to the backwater length, L_{bw}/L_s, and relative backwater rise due to ratio of jam upstream depth h_J to uniform flow depth h_0, based on jam physical structure:

$$\frac{h_J}{h_0} = \left(\frac{3\sqrt{3}\,SC_A}{2C_{f,0}}\right)^{1/3} \quad (1)$$

with slope S, jam structural metric $C_A = L_J C_D a_f/(1-\phi)^3$ is related to jam length L_J, drag coefficient for a rigid circular cylinder $C_D \cong 1$, frontal area density a_f, and solid volume fraction ϕ (Follett et al., 2020). Bed resistance in a wide channel assuming uniform flow without jams present ($C_{f,0} = gh_0^3S/q^2$) increases with the cube of uniform flow depth and can be related to Manning's resistance coefficient ($C_{f,0} = n_0^2 g/h_0^{1/3}$; Julien, 1998). For the relatively steep, forested catchments considered, Manning's n was found from slope ($n = 1.85S^{0.79}$ s m$^{-1/3}$) based on observations in high-gradient channels (Yochum et al., 2014). Relative backwater rise was high for most reaches, with $h_J/h_0 = 7 \pm 1.5$ (1σ) (solid circles, Figure 2a). Three sites with high unit bankfull discharge and lower ratio of average wood piece length to bankfull channel width also had lower $h_J/h_0 = 3.5, 3.5, 4.5$ (Figure 2a, dark green circles at lower right; Wohl & Iskin, 2022).

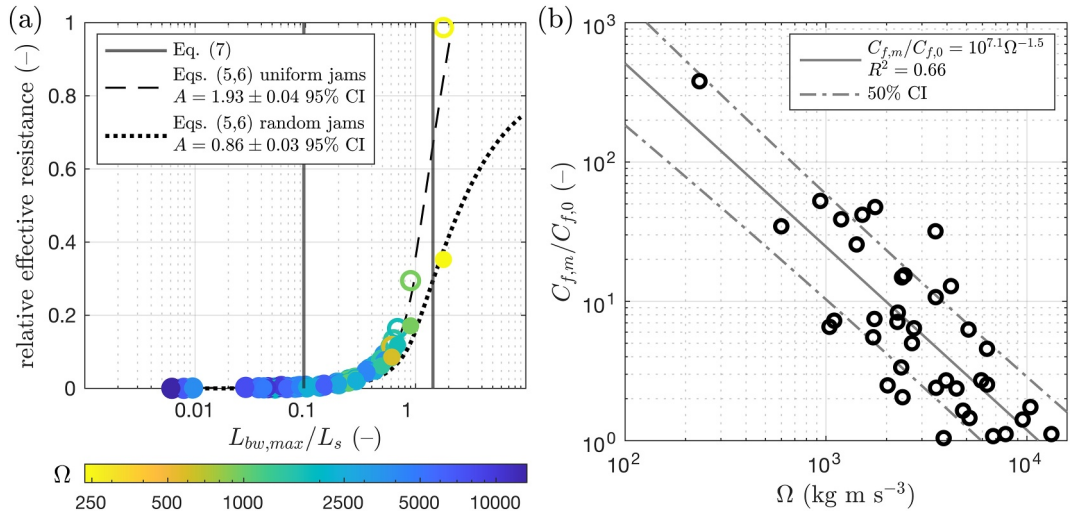

Figure 3. (a) Relative effective resistance $[(C_{f,m}-C_{f,0})/(C_{f,max}-C_{f,0})]$ increases with relative backwater rise h_J/h_0 and decreasing inter-jam spacing relative to maximum backwater length $L_{bw,max}/L_s$ at point of overtopping. Reaches with randomly distributed jams shown with filled circles. Reaches with uniform jam distribution shown with open circles. Decreasing stream power Ω shown by shift from blue to yellow circles. Color on log scale. (b) Best-fit resistance coefficient for a series of logjams relative to channel bed resistance decreases with stream power, shown with open black circles.

Jam occurrence followed a Poisson process linked to near-channel tree fall, which provided larger ramped wood pieces serving as jam key members, with additional contributions from fluvially transported wood (Beckman & Wohl, 2014; Wohl & Beckman, 2014; Wohl & Scamardo, 2021). Due to randomly distributed jam location at the reach scale (Wohl & Scamardo, 2021), distribution of inter-jam spacing distance from a jam to its nearest upstream or downstream neighbor follows an exponential distribution truncated between the minimum distance for two jams to be considered distinct (3 m) and the reach length, with probability density $f(x) = e^{-x/L_s}/\left(e^{-3/L_s} - e^{-L_R/L_s}\right)$ (solid black line, Figure 2b). Probability density of jam distance to nearest neighbors is shown in Figure 2b for 209 jam observations recorded over 11 years at an example site, Ouzel 2. For Ouzel 2, 59% of logjams would be expected to have a closer neighbor than the reach average ($x/L_s < 1$, Figure 2b), with some logjams spaced much further apart (15% $x/L_s > 2$, Figure 2b). For the cases considered here, upstream backwater depth depends only on unit discharge and jam structure, not water depth downstream of a jam ($q > q_c$, Follett et al., 2020). The presence of a backwater was not observed to promote or reduce jam presence, as jams were randomly distributed at the reach scale (Wohl & Scamardo, 2021). However, a close upstream neighbor reduces the effective jam backwater length, altering jam hydraulic impact. Maximum backwater length occurs at the point of overtopping when the upstream water surface is at the jam top edge ($h_J = H_J \cong H_{BF} = 0.65$ m in field observations). The probability of a jam occurring within $L_{bw,max}$ was

$$P(x \le L_{bw,max}) = 1 - e^{-L_{bw,max}/L_s}, \tag{2}$$

shown by filled circles with black outline in Figure 2c. Contours show $P(x \le L_{bw,max})$ for $H_{BF} = 0.65$ m, reach average $h_0/h_J = 0.14$, found from Equation 2 with approximate backwater length $L_{bw,max} = H_{BF}\,(1 - h_0/h_J)/S$.

3.2. Best-Fit Effective Resistance

To enable cross-reach comparison of jam structure and spacing for multiple logjams at the reach scale, an effective resistance coefficient was identified that minimized the sum of the squared difference in volume between outflow exiting a 1D channel containing a series of jams, and the same model channel with no jams present and effective resistance equal to $C_{f,m}$. Random (Wohl & Scamardo, 2021) and uniform jam distributions were compared for the same reach average jam density. Effective resistance increased from bed resistance in an unobstructed open channel $C_{f,0}$ (Figure 3a, $(C_{f,m}-C_{f,0})/(C_{f,max}-C_{f,0}) = 0$) to the theoretical maximum value $C_{f,max} = \frac{h_J^3 g S}{q^2}$, with $h = h_J$ everywhere in the channel (Figure 3a, $(C_{f,m}-C_{f,0})/(C_{f,max}-C_{f,0}) = 1$). Maximum inflow to the reach was equal to maximum backwater length $L_{bw,max}$ at the point of overtopping, with unit discharge

$q = \left[\frac{2g(H_{BF})^3}{3\sqrt{3}\,C_A}\right]^{1/2}$. Effective resistance increased primarily with L_{bw}/L_s (open and solid circles compared to dashed and dotted lines with constant $h_J/h_0 = 7$, Figure 3a). To aid in design of nature-based solutions using logjams, we approximated effective resistance (dashed and solid lines, Figure 3a) by assuming that $C_{f,m}$ is linearly proportional to the cube of segment-average water depth, $C_{f,m} \approx A\overline{h}_s^3$, with empirical constant A. For a channel segment containing one jam at the segment downstream edge, the segment-average water depth relative to h_0 was

$$\frac{\overline{h}_s}{h_0} = \begin{cases} 1 + \frac{L_{bw}}{L_s}\frac{1}{2}\left(\frac{h_J}{h_0} - 1\right), & L_{bw}/L_s \le 1 \\ \frac{h_J}{h_0} - \frac{1}{2}\frac{L_s}{L_{bw}}\left(\frac{h_J}{h_0} - 1\right), & L_{bw}/L_s > 1 \end{cases} \tag{3}$$

with increasing ratio of segment average to uniform depth dependent on relative jam spacing (L_{bw}/L_s) and backwater rise (h_J/h_0). To develop an analytical approximation, Equation 3 uses a simplified triangular backwater shape, while modeled effective resistance (Figure 3a) was found with an asymptotic backwater curve calculated iteratively (Chow, 1959; Julien, 1998). The relative increase in modeled effective resistance (Figure 3a) is then

$$\frac{C_{f,m} - C_{f,0}}{C_{f,max} - C_{f,0}} \cong \frac{A\left(\frac{\overline{h}_s}{h_0}\right)^3 - 1}{\left(\frac{h_J}{h_0}\right)^3 - 1}, \tag{4}$$

with empirical constant $A = 0.86 \pm 0.03$ for randomly distributed jams (Figure 3a, open circles) and $A = 1.93 \pm 0.04$ for uniform spacing (Figure 3a, solid circles) fit to model results. If $A > 1$, Equation 4 can yield a value greater than 1, which is not physically possible, so a restricted range of values $\frac{C_{f,m}-C_{f,0}}{C_{f,max}-C_{f,0}} \cong \min\left(\frac{A\left(\frac{\overline{h}_s}{h_0}\right)^3 - 1}{\left(\frac{h_J}{h_0}\right)^3 - 1}, 1\right)$ should be used. By expanding Equation 4 with the definitions in Equation 3, we obtain:

$$\frac{\frac{C_{f,m}}{C_{f,0}} - 1}{\frac{C_{f,max}}{C_{f,0}} - 1} \cong \frac{A\left(1 + \frac{3}{2}\frac{L_{bw}}{L_s}\left(\frac{h_J}{h_0} - 1\right) + \frac{3}{4}\left(\frac{L_{bw}}{L_s}\right)^2\left(\frac{h_J}{h_0} - 1\right)^2 + \frac{1}{8}\left(\frac{L_{bw}}{L_s}\right)^3\left(\frac{h_J}{h_0} - 1\right)^3\right) - 1}{\left(\frac{h_J}{h_0}\right)^3 - 1} \tag{5}$$

for $L_{bw}/L_s \le 1$, and

$$\frac{\frac{C_{f,m}}{C_{f,0}} - 1}{\frac{C_{f,max}}{C_{f\cong 0}} - 1} \cong \frac{A\left(\left(\frac{h_J}{h_0}\right)^3 - \frac{3}{2}\frac{L_{bw}}{L_s}\left(\frac{h_J}{h_0}\right)^2\left(\frac{h_J}{h_0} - 1\right) + \frac{3}{4}\left(\frac{L_{bw}}{L_s}\right)^2\left(\frac{h_J}{h_0}\right)\left(\frac{h_J}{h_0} - 1\right)^2 - \frac{1}{8}\left(\frac{L_{bw}}{L_s}\right)^3\left(\frac{h_J}{h_0} - 1\right)^3\right) - 1}{\left(\frac{h_J}{h_0}\right)^3 - 1} \tag{6}$$

when $L_{bw}/L_s > 1$. Equations 5 and 6 describe a polynomial approximating the increase in best-fit effective resistance corresponding to a series of jams with spacing L_{bw}/L_s and relative increase in backwater rise h_J/h_0 (Figure 3a, dotted and dashed black lines). For a jam with a given h_J/h_0, steepest increase in resistance occurs when the cubic terms of Equations 5 and 6 are of comparable magnitude to the linear and quadratic terms:

$$\frac{L_{bw}}{L_s} = \frac{6}{10\left(\frac{h_J}{h_0} - 1\right)}, \frac{10\left(\frac{h_J}{h_0} - 1\right)}{6\frac{h_J}{h_0}}, \tag{7}$$

as shown in Figure 3a with vertical solid black lines. Equation 7 could be used to target jam placement to the range in which the highest rate of increase in effective resistance with increasing jam density is observed. For the conditions considered, the rate of increase in effective resistance was reduced for jams with an upstream neighbor

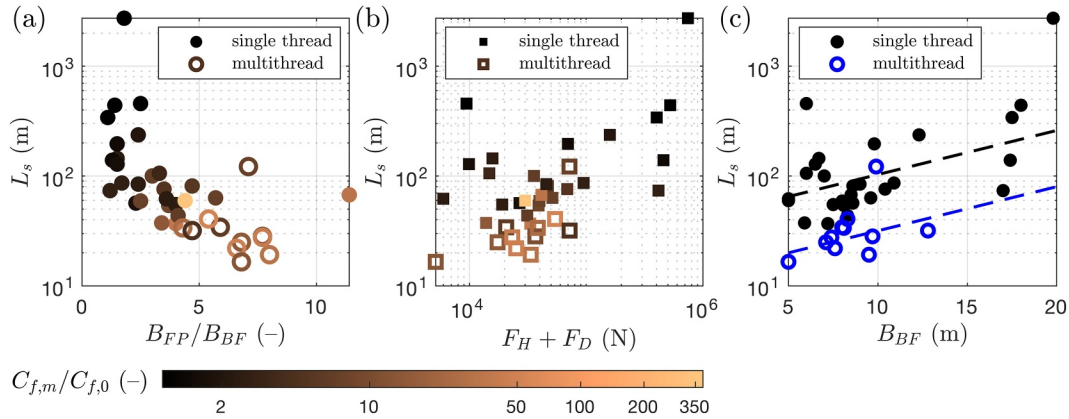

Figure 4. (a) Reach average inter-jam spacing with ratio of floodplain width to channel width. (b) Reach average inter-jam spacing with hydrostatic and dynamic force on jam with discharge equal to bankfull discharge ($Q = Q_{BF}$). (c) Reach average spacing between jams with bankfull channel height. Linear relationships for single thread and multithread sites shown with dashed black ($L_s = 13B_{BF}$ 95%CI 9–18, Matlab *REGRESS* excluding low density site ($B_{BF} = 19.8$, $L_s = 2{,}732$)) and blue ($L_s = 4B_{BF}$, 95%CI 2–6) lines.

within one backwater length, because the backwater extended only over the local inter-jam spacing $L_{s,i} < L_{bw}$, reducing the impact per jam. The difference between uniform and random jam distribution became more pronounced at higher relative jam densities, due to increasing frequency of backwater truncation (Figure 3c), until the curves converged at very high jam density. For the sites considered here, difference between random and uniform reaches was greater than 5% of variation between uniform and maximum $[(C_{f,m}-C_{f,0})/(C_{f,max}-C_{f,0}) = 0.05]$ for $L_{bw}/L_s > 0.7$.

The effective resistance increases with cubic equations related to relative backwater rise h_J/h_0 and jam density L_{bw}/L_s (Equations 5 and 6, black dashed and dotted curves in Figure 3a). Effective resistance at the point of overtopping decreased with increasing stream power $\Omega = \rho g q_{BF} B_{BF} S$ (kg m s^{-3}) ($C_{f,m}/C_{f,0} = 10^{5.3}\ \Omega^{-1.3}$, $R^2 = 0.63$ for randomly distributed jams, gray line in Figure 3b), due to decrease of relative jam density with increasing slope ($L_{bw} \sim S^{-1}$) and bankfull channel width ($L_s^{-1} = 0.31 B_{BF}^{-1.44}, R^2 = 0.25$), and decrease of h_J/h_0 with bankfull unit discharge ($h_J/h_0 = 5.3 q_{BF}^{-0.47}, R^2 = 0.31$, Figure 2a) and channel width due to decreasing L_w/B_{BF} ($h_J/h_0 = 13.5 B_{BF}^{-0.3}, R^2 = 0.21$).

3.3. Relationship of Reach-Average Spacing to Floodplain Properties and Jam Lifetime

For the reaches in this study, jam formation and persistence, which increased jam spatial density L_s^{-1}, reflected two-way interaction with the local floodplain in addition to channel characteristics (Figure 4a). The channel-spanning jams in this study were observed to create a visible backwater at base flow. Individual jam porosity varied between jams and year to year. In general, jams had relatively low porosity, approximately 5%–10%. The point of jam overtopping occurred at $Q/Q_{BF} = 0.06 \pm 0.03$, indicating that channel-floodplain reconnection commonly occurred in the jam backwater. Observed jam spatial density primarily increased with ratio of floodplain width to channel width, with ratio of log length to channel width and multichannel planform also considered significant (Wohl & Scamardo, 2021). Sites with multithread planform tended to occur in less confined reaches (Figure 4a, open black circles; $B_{fp}/B \geq 2$, Wohl & Iskin, 2022; Marshall & Wohl, 2023).

The reduced lateral confinement of overbank flows allows water to spread out over a wider floodplain area, increasing energy dissipation within the floodplain and reducing water depth compared to the same discharge in a confined reach. The hydrostatic (F_H) and dynamic (F_D) forces on a jam at $Q = Q_{BF}$ were estimated from upstream water depth and channel velocity (Julien, 1998; Manners et al., 2007),

$$F_H = \rho g (h_J - h_0) A_J \tag{8}$$

$$F_D = \frac{1}{2} \rho U_{BF,J}^2 A_J \tag{9}$$

assuming that $A_J = B_{BF}H_{BF}$, water spatial average water velocity at the jam face equal to velocity at the point of overtopping $U_{BF,J} = q_{BF,J}/H_{BF}$, water depth equal between channel and floodplain sections, flow over jam ($H_J = H_{bf}$) followed a sharp-crested weir (Follett and Hankin, 2022; Supporting Information S1), and flow on the floodplain followed uniform flow with Manning's $n = 0.1$. Reach-average jam spacing increased with hydrostatic and dynamic force (Figure 4b). For the same estimated force, multithread reaches (Figure 4b, open squares) had 3.4 times higher jam density than single-thread reaches (solid and open squares in Figure 4b), suggesting that multithread reaches promoted jam density in addition to the effect of valley confinement. This is consistent with regression model results indicating that a multichannel planform is an additional predictor of jam density (Wohl & Scamardo, 2021). However, median and variance of logjam persistence was not found to differ between multithread and single-thread reaches (see Text S2 and Figure S1 in Supporting Information S1). The probability density function of jam lifetime followed a Weibull distribution with decreasing hazard function, indicating that a jam observed in a given year that was already present in prior surveys was more likely to survive and be counted the following year than a newly formed jam.

4. Discussion

Modeled effective resistance increased with extent of increase in flow depth upstream of the logjam and logjam spacing relative to backwater length (Figure 3). Similarly, Wilcox and Wohl (2006) measured increase in friction factor for model reaches with wood pieces in experimental flume studies, finding that wood piece density strongly influences flow resistance to a greater extent than varying piece orientation, length, or arrangement. Across the range of study sites (Figure 1), effective resistance was 1.04–380 times channel resistance without logjams, with median value $C_{f,m}/C_{f,0} = 5.90$ (Figures 4a and 4b, black to brown markers). Linstead and Gurnell (1999) used tracer measurements to obtain the increase in reach scale Manning's n for in-channel flows in two reaches in the Forest of Dean, an ancient mixed woodland (Gloucestershire, UK) including channel-spanning logjams with a visible backwater rise at base flow. The observed increase due to channel-spanning jams was equivalent to $C_f/C_{f,0} = 4$, within the broad range of model results for this study, despite the different geographic context (Linstead & Gurnell, 1999). Existing guidance for placement of manmade wood jams (Wren et al., 2022; YDRT, 2021) suggests $L_s = 7B_{BF}$, based on $L_s = 7$–$10\ B_{BF}$ observed in the Forest of Dean (Linstead & Gurnell, 1999). Reaches in this study with a multithread planform had higher jam density ($L_s = 4B_{BF}$, 95%CI 2–6, blue dashed line in Figure 4c) than single-thread reaches ($L_s = 13B_{BF}$, 95%CI 9–18, black dashed line in Figure 4c). Logjam density could have increased above that observed in most reaches while remaining within the region of steepest increase ($L_s = 0.8B_{BF}$, 95%CI 0.5–1.2). Project designers could target jam densities within the range given by Equation 7 to provide higher value for money.

Addition of wood pieces and wood barriers such as beaver dam analogs and engineered logjams often occurs with the aim of enhancing hydraulic and geomorphic complexity, in addition to promoting water storage and enhancing flood mitigation (Bouwes et al., 2018). The UK River Condition Assessment recognizes floodplain geomorphic complexity including side channels and ponds as well as presence of in-channel individual wood pieces in promoting biodiversity (Gurnell et al., 2020). Individual wood pieces locally increase flow heterogeneity, but typically have lower impact on upstream backwater rise (<5%, Gippel et al., 1996) than the channel-spanning logjams considered here. In this study, median $C_{f,m}/C_{f,0}$ was higher at multithread ($C_{f,m}/C_{f,0} = 15$) than single-thread sites ($C_{f,m}/C_{f,0} = 3$). However, single-thread sites had a broad range of $C_{f,m}/C_{f,0}$, both higher and lower than that observed for multithread sites. These results consider only in-channel flows, similar to prior observations of increase in channel roughness due to logjams (Linstead & Gurnell, 1999). Due to the role of logjams in enhancing geomorphic complexity, we suggest further work is needed both to link real-world increase reach scale roughness with logjam structure and spacing and to characterize the role of logjams in overbank flow conditions.

5. Conclusion

We compared logjam structure and spacing across 37 reaches observed over 11 years in the Colorado Rockies. This unmanaged system provides an ideal data set to explore how logjam presence is related to channel characteristics such as channel slope, channel bankfull width and depth, bed resistance, and valley confinement. To enable cross-reach comparison of multiple logjams at the reach scale, we identified best-fit elevated effective resistance which generated an outflow hydrograph that most closely matched the outflow from a model reach

containing a series of individual logjams. Effective resistance increased with relative backwater rise h_J/h_0, linked to jam physical structure, and relative jam density L_{bw}/L_s, linked to reach-average jam spacing (Figure 3a). Consistent with these mechanisms, effective resistance increased with decreasing stream power (Figure 3c). The region of strongest increase in effective resistance occurred between boundaries dependent on h_J/h_0, (Equation 7), and can be approximated analytically (Equations 5 and 6). Wood enhancement and engineered logjam projects could target this region to maximize value for money and estimate the magnitude of impact on elevated effective resistance. For the same reach-average jam density, randomly distributed jams (Wohl & Scamardo, 2021) had reduced effective resistance relative to a uniform jam distribution, due to occurrence of jams spaced within L_{bw} (Figures 2b and 2c), which reduced the effect of individual backwaters truncated by close upstream neighbors. In addition to channel characteristics, jam formation and persistence also depends on overbank flows, with observed jam density linked to decreasing valley confinement (Figure 4a, Wohl & Scamardo, 2021). A decrease in hydrostatic and dynamic force on the logjam at bankfull discharge due to reduced valley confinement was consistent with increasing jam density (Figure 4b). We suggest further work is needed to characterize the interaction between logjams and floodplain flows, including influence of increased reconnection provided by jam backwaters on floodplain vegetation and maintenance of multiple channels, and impact of overbank flows on jam stability.

Data Availability Statement

Data can be freely accessed via Colorado State University's Mountain Scholar and are available in Supporting Information S1 files of Wohl and Scamardo (2021) and Wohl and Iskin (2022). The 1D network model file presented in this paper is available at Follett (2024). Model parameters and field data are available at Wohl & Follett (2024).

Acknowledgments
The first author has received funding from the Royal Academy of Engineering's Research Fellowships programme. We thank Rocky Mountain National Park for permission to conduct field-based research in the park.

References

Addy, S., & Wilkinson, M. (2019). Representing natural and artificial in-channel large wood in numerical hydraulic and hydrological models. *WIREs Water*, *6*, e139. https://doi.org/10.1002/wat2.1389

Beckman, N. (2013). Crossing a threshold: The legacy of 19th century logging on log Jams and carbon storage in front range headwater streams. In *PhD dissertation*. Colorado State University.

Beckman, N. D., & Wohl, E. (2014). Effects of forest stand age on the characteristics of logjams in mountainous forest streams. *Earth Surface Processes and Landforms*, *39*(11), 1421–1431. https://doi.org/10.1002/esp.3531

Bilby, R. (1981). Role of organic debris dams in regulating the export of dissolved and particulate matter from a forested watershed. *Ecology*, *62*(5), 1234–1243. https://doi.org/10.2307/1937288

Bouwes, N., Weber, N., Jordan, C., Saunders, W., Tattam, I., Volk, C., et al. (2018). Ecosystem experiment reveals benefits of natural and simulated beaver dams to a threatened population of steelhead (Oncorhynchus mykiss). *Scientific Reports*, *6*(1), 28581. https://doi.org/10.1038/srep28581

Brown, G., Lespez, L., Sear, D., Macaire, J., Houben, P., Klimek, K., et al. (2018). Natural vs anthropogenic streams in Europe: History, ecology and implications for restoration, river-rewilding and riverine ecosystem services. *Earth-Science Reviews*, *180*, 185–205. https://doi.org/10.1016/j.earscirev.2018.02.001

Brummer, C., Abbe, T., Sampson, J., & Montgomery, D. (2006). Influence of vertical channel change associated with wood accumulations on delineating channel migration zones, Washington, USA. *Geomorphology*, *80*(3–4), 295–309. https://doi.org/10.1016/j.geomorph.2006.03.002

Chow, V. T. (1959). *Open-channel hydraulics*. McGraw-Hill.

Collins, B., Montgomery, D., Fetherston, K., & Abbe, T. (2012). The floodplain large-wood cycle hypothesis: A mechanism for the physical and biotic structuring of temperate forested alluvial valleys in the North Pacific coastal ecoregion. *Geomorphology*, *139–40*, 460–470. https://doi.org/10.1016/j.geomorph.2011.11.011

Collins, B., Montgomery, D., & Haas, A. (2002). Historical changes in the distribution and functions of large wood in Puget Lowland Rivers. *Canadian Journal of Fisheries and Aquatic Sciences*, *59*(1), 66–76. https://doi.org/10.1139/f01-199

Collins, B., Montgomery, D., & Sheikh, A. (2003). Reconstructing the historical riverine landscape of the Puget lowland. In D. Montgomery, S. Bolton, D. Booth, & L. Wall (Eds.), *Restoration of puget sound rivers* (pp. 79–128). University of Washington Press.

Deane, A., Norrey, J., Coulthard, E., McKendry, D., & Dean, A. (2021). Riverine large woody debris introduced for natural flood management leads to rapid improvement in aquatic macroinvertebrate diversity. *Ecological Engineering*, *163*, 106197. https://doi.org/10.1016/j.ecoleng.2021.106197

Follett (2024). efollett/effective-resistance: Release 1 (Version v1) [Software]. *Zenodo*. https://doi.org/10.5281/zenodo.11111139

Follett, E., & Hankin, B. (2022). Investigation of effect of logjam series for varying channel and barrier physical properties using a sparse input data 1D network model. *Environmental Modelling & Software*, *158*, 105543. https://doi.org/10.1016/j.envsoft.2022.105543

Follett, E., Schalko, I., & Nepf, H. (2020). Momentum and energy predict the backwater rise generated by a large wood jam. *Geophysical Research Letters*, *47*(17), e2020GL089346. https://doi.org/10.1029/2020GL089346

Gippell, C. J., O'Neill, I. C., Finlayson, B. L., & Schnatz, I. (1996). Hydraulic guidelines for the re-introduction and management of large woody debris in lowland rivers. *Regulated Rivers: Research & Management*, *12*(2–3), 223–236. https://doi.org/10.1002/(sici)1099-1646(199603)12:2/3<223::aid-rrr391>3.0.co;2-#

Grabowski, R., Gurnell, A., Burgess-Gamble, L., England, J., Holland, D., Klaar, M., et al. (2019). The current state of the use of large wood in river restoration and management. *Water and Environment Journal*, *33*(3), 366–377. https://doi.org/10.1111/wej.12465

Gregory, S., Boyer, K., & Gurnell, A. (Eds.) (2003). *The ecology and management of wood in world rivers*. American Fisheries Society.

Gurnell, A., Scott, S., England, J., Gurnell, D., Jeffries, R., Shuker, L., & Wharton, G. (2020). Assessing river condition: A multiscale approach designed for operational application in the context of biodiversity net gain. *River Research and Applications*, *36*(8), 1559–1578. https://doi.org/10.1002/rra.3673

Gurnell, A., Tockner, K., Edwards, P., & Petts, G. (2005). Effects of deposited wood on biocomplexity of river corridors. *Frontiers in Ecology and the Environment*, *3*(7), 377–382. https://doi.org/10.1890/1540-9295(2005)003[0377:EODWOB]2.0.CO;2

Julien, P. (1998). *Erosion and sedimentation*. Cambridge University Press.

Linstead, C., & Gurnell, A. M. (1999). *Large woody debris in British headwater rivers: Physical habitat role and management guidelines*. Environment Agency R & D Technical Report W185. https://assets.publishing.service.gov.uk/government/uploads/system/uploads/attachment_data/file/290559/str-w185-e-e.pdf

Livers, B., & Wohl, E. (2015). An evaluation of stream characteristics in glacial versus fluvial process domains in the Colorado Front Range. *Geomorphology*, *231*, 72–82. https://doi.org/10.1016/j.geomorph.2014.12.003

Livers, B., & Wohl, E. (2021). All logjams are not created equal. *Journal of Geophysical Research: Earth Surface*, *126*(8), e2021JF006076. https://doi.org/10.1029/2021JF006076

Livers, B., Wohl, E., Jackson, K., & Sutfin, N. (2017). Historical land use as a driver of alternative states for stream form and function in forested mountain watersheds of the Southern Rocky Mountains. *Earth Surface Processes and Landforms*, *43*(3), 669–684. https://doi.org/10.1002/esp.4275

Livers Gonzalez, B. (2016). Instream wood loads and channel complexity in headwater southern Rocky Mountain streams under alternative states. In *PhD dissertation*. Colorado State University.

Manners, R., Doyle, M., & Small, M. (2007). Structure and hydraulics of natural woody debris jams. *Water Resources Research*, *43*(6), W06432. https://doi.org/10.1029/2006WR004910

Mao, L., Andreoli, A., Comiti, M., & Lenzi, A. (2008). Geomorphic effects of large wood jams on a sub-antarctic mountain stream. *River Research and Applications*, *24*(3), 249–266. https://doi.org/10.1002/rra.1062

Marshall, A., & Wohl, E. (2023). The continuum of wood-induced channel bifurcations. *Frontiers in Water*, *5*, 1155623. https://doi.org/10.3389/frwa.2023.1155623

Montgomery, D., & Buffington, J. (1997). Channel-reach morphology in mountain drainage basins. *GSA Bulletin*, *109*(5), 596–611. https://doi.org/10.1130/0016-7606(1997)109<0596:CRMIMD>2.3.CO;2

Montgomery, D., Collins, B., Buffington, J., & Abbe, T. (2003). Geomorphic effects of wood in rivers. In S. Gregory, K. Boyer, & A. Gurnell (Eds.), *The ecology and management of wood in World Rivers*. American Fisheries Society.

Pess, G., Liermann, M., McHenry, M., Peters, R., & Bennett, T. (2011). Juvenile salmon response to the placement of engineered log jams (ELJs) in the Elwha River, Washington State, USA. *River Research and Applications*, *28*(7), 872–881. https://doi.org/10.1002/rra.1481

Pišút, P. (2002). Channel evolution of the pre-channelized Danube River in Bratislava, Slovakia (1712–1886). Earth surface processes and. *Landforms*, *27*(4), 369–390. https://doi.org/10.1002/esp.333

Polvika, C., & Claeson, S. (2020). Beyond redistribution: In-stream habitat restoration increases capacity for young-of-the-year chinook salmon and steelhead in the Entiat River, Washington. *North American Journal of Fisheries Management*, *40*(2), 446–458. https://doi.org/10.1002/nafm.10421

Roni, P., Beechie, T., Pess, G., & Hanson, K. (2015). Wood placement in river restoration: Fact, fiction, and future direction. *Canadian Journal of Fisheries and Aquatic Sciences*, *72*(3), 466–478. https://doi.org/10.1139/cjfas-2014-0344

Ruiz-Villanueva, V., Piégay, H., Gurnell, A. M., Marson, R., & Stoffel, M. (2016). Recent advances quantifying the large wood dynamics in river basins: New methods and remaining challenges. *Reviews of Geophysics*, *54*(3), 611–752. https://doi.org/10.1002/2015RG000514

Schalko, I., Schmocker, L., Weitbrecht, V., & Boes, R. (2018). Backwater rise due to large wood accumulations. *Journal of Hydraulic Engineering*, *144*(9), 04018056. https://doi.org/10.1061/(ASCE)HY.1943-7900.0001501

Sear, D. A., Millington, C. E., Kitts, D. R., & Jeffries, R. (2010). Logjam controls on channel: Flood plain interactions in wooded catchments and their role in the formation of multi-channel patterns. *Geomorphology*, *116*(3–4), 305–319. https://doi.org/10.1016/j.geomorph.2009.11.022

Swanson, F. J., Gregory, S. V., Iroumé, A., & Ruiz-Villanueva, V. (2020). Recent advances quantifying the large wood dynamics in river basins: New methods and remaining challenges. *Reviews of Geophysics*, *54*(3), 611–652. https://doi.org/10.1002/esp.4814

Welling, R. T., Wilcox, A. C., & Dixon, J. L. (2021). Large wood and sediment storage in a mixed bedrock-alluvial stream, western Montana, USA. *Geomorphology*, *384*(1), 107703. https://doi.org/10.1016/j.geomorph.2021.107703

Wilcox, A., & Wohl, E. (2006). Flow resistance dynamics in step-pool stream channels: 1. Large woody debris and controls on total resistance. *Water Resources Research*, *42*(5), W05418. https://doi.org/10.1029/2005WR004277

Wohl, E. (2011). Threshold-induced complex behavior of wood in mountain streams. *Geology*, *39*(6), 587–590. https://doi.org/10.1130/G32105.1

Wohl, E. (2014). A legacy of absence: Wood removal in US rivers. *Progress in Physical Geography: Earth and Environment*, *38*(5), 637–663. https://doi.org/10.1177/0309133314548091

Wohl, E. (2017). Bridging the gaps: An overview of wood across time and space in diverse rivers. *Geomorphology*, *279*, 3–26. https://doi.org/10.1016/j.geomorph.2016.04.014

Wohl, E., & Beckman, N. (2014). Controls on the longitudinal distribution of channel-spanning logjams in the Colorado Front Range. *USA. River Research and Applications*, *30*(1), 112–131. https://doi.org/10.1002/rra.2624

Wohl, E., Bledsoe, B. P., Fausch, K. D., Kramer, N., Bestgen, K. R., & Gooseff, M. N. (2016). Management of large wood in streams: An overview and proposed framework for hazard evaluation. *Journal of the American Water Resources Association*, *52*(2), 315–335. https://doi.org/10.1111/1752-1688.12388

Wohl, E., & Follett, E. (2024). Dataset: Reach characteristics and best-fit effective resistance [Dataset]. *Zenodo*. https://doi.org/10.5281/zenodo.11111158

Wohl, E., & Iskin, E. (2022). The transience of channel-spanning logjams in mountain streams. *Water Resources Research*, *58*(5), e2021WR031556. https://doi.org/10.1029/2021WR031556

Wohl, E., & Scamardo, J. (2021). The resilience of logjams to floods. *Hydrological Processes*, *35*(1), e13970. https://doi.org/10.1002/hyp.13970

Wren, E., Barnes, M., Janes, M., Kitchen, A., Nutt, N., Patterson, C., et al. (2022). *The natural flood management manual*. CIRIA.

Yochum, S. E., Comiti, F., Wohl, E., David, G. C. L., & Mao, L. (2014). Photographic guidance for selecting flow resistance coefficients in high-gradient channels. In *General technical report No. RMRS-GTR-323* (p. 91). U.S. Department of Agriculture, Forest Service, Rocky Mountain Research Station. https://doi.org/10.2737/RMRS-GTR-323

Yorkshire Dales Rivers Trust. (2021). Naturally resilient: Leaky dams. Retrieved from https://www.ydrt.org.uk/wp-content/uploads/2021/04/NFM-Leaky-Dams-guide.pdf

AGU ADVANCING EARTH AND SPACE SCIENCES

Geophysical Research Letters®

16 September 2024 · Volume 51 · Issue 17

WILEY

Geophysical Research Letters®

AN AGU JOURNAL

Publisher. *Geophysical Research Letters,* ISSN 0094-8276, is published semi-monthly on behalf of the American Geophysical Union by Wiley Periodicals LLC, 111 River St., Hoboken, NJ, 07030-5774 USA, +1 201 748 6000.

Journal Customer Services. For institutional subscription information, claims and any enquiry concerning your journal subscription please go to www.wileycustomerhelp.com/ask or contact your nearest office.

Americas: Email: cs-journals@wiley.com; Tel: +1 781 388 8598 or +1 800 835 6770 (toll free in the USA & Canada).
Europe, Middle East and Africa: Email: cs-journals@wiley.com; Tel: +44 (0) 1865 778315.
Asia Pacific: Email: cs-journals@wiley.com; Tel: +65 6511 8000.
Japan: For Japanese speaking support, Email: cs-japan@wiley.com; Tel: +65 6511 8010 or Tel (toll-free): 005 316 50 480.

Visit our Online Customer Help at https://wolsupport.wiley.com/s/contact-support?tabset-a7d10=2

Production Editor. For assistance with post-acceptance articles and other production issues please contact GRLprod@wiley.com.

Access to this journal is available free online within institutions in the developing world through the AGORA initiative with the FAO, the HINARI initiative with the WHO, the OARE initiative with UNEP, and the ARDI ini-tiative with WIPO. For information, visit www.aginternetwork.org, www.who.int/hinari/en/, www.oaresciences.org, or www.wipo.int/ardi/en.

For submission instructions, subscription and all other information visit: http://grl.agu.org

Cover: In Follett & Wohl. (https://doi.org/10.1029/2024GL110126), downstream face of channel-spanning logjam on Reach 1 of Hunter's River, Rocky Mountain National Park, Colorado. We compare logjam structure and spacing at the reach scale by identifying a modelled best-fit effective resistance coefficient. Effective resistance due to logjams increases most strongly for intermediate jam density, dependent on ratio of jam upstream depth to depth without a logjam and ratio of backwater length to average spacing. e2024GL110126. Credit: Professor Ellen Wohl.